Journal of Dental Research
2015, Vol. 94(9) 1303–1309
© International & American Associations for Dental Research 2015
Reprints and permissions: sagepub.com/journalsPermissions.nav
DOI: 10.1177/0022034515589284
jdr.sagepub.com

Removal of Dental Biofilms with an Ultrasonically Activated Water Stream

R.P. Howlin[1,2], S. Fabbri[3], D.G. Offin[4], N. Symonds[3], K.S. Kiang[5], R.J. Knee[2], D.C. Yoganantham[2], J.S. Webb[1,2], P.R. Birkin[4], T.G. Leighton[6,7], and P. Stoodley[3,8]

Abstract

Acidogenic bacteria within dental plaque biofilms are the causative agents of caries. Consequently, maintenance of a healthy oral environment with efficient biofilm removal strategies is important to limit caries, as well as halt progression to gingivitis and periodontitis. Recently, a novel cleaning device has been described using an ultrasonically activated stream (UAS) to generate a cavitation cloud of bubbles in a freely flowing water stream that has demonstrated the capacity to be effective at biofilm removal. In this study, UAS was evaluated for its ability to remove biofilms of the cariogenic pathogen *Streptococcus mutans* UA159, as well as *Actinomyces naeslundii* ATCC 12104 and *Streptococcus oralis* ATCC 9811, grown on machine-etched glass slides to generate a reproducible complex surface and artificial teeth from a typodont training model. Biofilm removal was assessed both visually and microscopically using high-speed videography, confocal scanning laser microscopy (CSLM), and scanning electron microscopy (SEM). Analysis by CSLM demonstrated a statistically significant 99.9% removal of *S. mutans* biofilms exposed to the UAS for 10 s, relative to both untreated control biofilms and biofilms exposed to the water stream alone without ultrasonic activation ($P < 0.05$). The water stream alone showed no statistically significant difference in removal compared with the untreated control ($P = 0.24$). High-speed videography demonstrated a rapid rate (151 mm^2 in 1 s) of biofilm removal. The UAS was also highly effective at *S. mutans, A. naeslundii*, and *S. oralis* biofilm removal from machine-etched glass and *S. mutans* from typodont surfaces with complex topography. Consequently, UAS technology represents a potentially effective method for biofilm removal and improved oral hygiene.

Keywords: bacteria, caries, dental hygiene, infection control, microbiology, *Streptococcus mutans*

Introduction

The oral cavity provides an optimal environment for the colonization and proliferation of a diverse array of microorganisms (Aas et al. 2005; Zaura et al. 2009). The most prevalent are bacteria, which exist primarily as a biofilm, commonly known as dental plaque, on the tooth surface. The accumulation of dental biofilm plays a key role in the pathogenesis of a range of oral diseases, including gingivitis, periodontitis, and caries (Aspiras et al. 2010).

Streptococcus mutans is a major cariogenic constituent of the supragingival biofilm due, in part, to its ability to grow and metabolize optimally at low pH (von Ohle et al. 2010). This gives it the ability to outcompete noncariogenic commensal species, thus altering microbial homeostasis in favor of the proliferation of acidogenic and aciduric microbial species and the establishment of a disease state (Marsh 2003; Falsetta et al. 2012; Lemos et al. 2013). Most control strategies, therefore, focus on preventing the proliferation of dental biofilm through frequent removal by mechanical oral hygiene procedures, usually in combination with chemical detrifrices (Brading and Marsh 2003; Forssten et al. 2010; Marsh 2010). However, even with good oral hygiene practices, such as regular brushing, flossing, water jets, and high-velocity water drops, biofilms can still accumulate on hard-to-reach places on the tooth surface.

Studies have previously demonstrated that the passage of a water-air interface over a solid surface can entrain bacteria and

[1]National Institute for Health Research Southampton Respiratory Biomedical Research Unit, Southampton Centre for Biomedical Research, University Hospital Southampton NHS Foundation Trust, Southampton, UK
[2]Centre for Biological Sciences, Faculty of Natural and Environmental Sciences and Institute for Life Sciences, University of Southampton, Southampton, UK
[3]National Centre for Advanced Tribology, Faculty of Engineering and Institute for Life Sciences, University of Southampton, Southampton, UK
[4]Chemistry, University of Southampton, Southampton, UK
[5]Southampton Nanofabrication Centre Electronics & Computer Science, University of Southampton, Southampton, UK
[6]Faculty of Engineering and the Environment, University of Southampton, Southampton, UK
[7]Institute of Sound and Vibration Research, University of Southampton, Southampton, UK
[8]Departments of Microbial Infection and Immunity and Orthopaedics, Center for Microbial Interface Biology, The Ohio State University, Columbus, OH, USA

A supplemental appendix to this article is published electronically only at http://jdr.sagepub.com/supplemental.

Corresponding Author:
P. Stoodley, Center for Microbial Interface Biology, The Ohio State University, 716 Biomedical Research Tower, 460 West 12th Ave, Columbus, OH 43210, USA.
Email: pstoodley@gmail.com

provide effective biofilm cleaning (Gomez-Suarez et al. 2001; Parini and Pitt 2006). This can be achieved with the passage of a microbubble stream, occasionally combined with ultrasonic agitation, to generate significant surface tension and shear forces for mechanical-based cleaning (Parini and Pitt 2005; Halford et al. 2012). Recently, a novel cleaning system has been developed that uses the acoustic activation of bubbles within a free flow of water to generate an ultrasonically activated stream (UAS) (Leighton et al. 2011). The forces acting on individual gas bubbles cause them to coalesce and move over the surface or be trapped within pits and fissures within the substratum (Leighton 1994; Doinikov 2001; Stricker et al. 2013), where the motion and cavitation dynamics of the bubbles create local shear and pressure, contributing to cleaning efficacy (Rooney 1970). This has been demonstrated in oral models (Leighton 1994; O'Leary et al. 1997; Lea et al. 2005) using standard dental ultrasonic equipment but never with contact-free technologies such as UAS. Particularly with respect to the pits and recesses of a surface, the entrapment of dynamic gas bubbles produces highly effective cleaning that may not be achieved with a normal water stream (Offin et al. 2014). This study aims to evaluate the efficacy of UAS as a novel approach to dental biofilm removal.

Materials and Methods

Bacteria and Biofilm Growth Conditions

Overnight cultures of *S. mutans* UA159 (ATCC 700610), *Actinomyces naeslundii* ATCC 12104, and *Streptococcus oralis* ATCC 9811 were grown in brain heart infusion (BHI; Sigma-Aldrich, St. Louis, MO, USA) broth at 37 °C (for *S. mutans*, BHI was supplemented with 2% sucrose [Sigma-Aldrich] and cultures were grown at 5% CO_2). Each culture was diluted in fresh media to an optical density value corresponding to 10^6 colony-forming units (CFU)/mL. The adjusted culture was used as an inoculum to assess UAS cleaning on a variety of increasingly complex surfaces with different roughness and material properties. Biofilms were grown on all surfaces for 72 h at 37 °C (with 5% CO_2 for *S. mutans* biofilm growth) in a humidified incubator with media changes performed every 24 h.

The UAS Device

We used a benchtop prototype of the StarStream UAS device (Leighton 2011) (Ultrawave Precision Ultrasonic Cleaning Equipment, Cardiff, UK). The device generates a stream of water at 2.1 L/min (±0.2 L/min) from a 10-mm diameter circular orifice, down which an ultrasonic field is projected. The device also creates bubble clouds, which impinge on the sample and spread laterally, and clean from the shear they generate (Leighton 1994). Biofilms were positioned 1 cm downstream from the orifice and exposed to a continuous stream of UAS for 10 s at room temperature.

Removal of Biofilms from Flat Surfaces Using an UAS

Glass slides were sterilized by autoclaving at 121 °C for 20 min. The slides were immersed vertically in a tube containing 40 mL of a 10^6 CFU/mL culture of either *S. mutans, A. naeslundii*, or *S. oralis*, and biofilms were grown as described above.

Following UAS exposure with the water stream positioned perpendicular to the surface, the slides were fluorescently stained with Live/Dead Baclight (Invitrogen, Carlsbad, CA, USA) in the dark for 20 min. Following a rinse in Hank's buffered salt solution (HBSS; Sigma-Aldrich) for 5 s, the slides were imaged using an inverted Leica DMI600 SP5 confocal scanning laser microscope (CSLM; Leica Microsystems, Milton Keynes, UK). Image analysis was carried out using the image analysis package COMSTAT (www.comstat.dk) (Heydorn et al. 2000). Assays were performed in duplicate (n = 4 image stacks per repeat) and statistical analysis performed using the Mann-Whitney rank sum tests for nonnormally distributed data and difference considered significant where $P < 0.05$.

In addition, *S. mutans* biofilms were grown in 9-cm, presterilized Petri dishes as described above. The UAS device was positioned centrally over the Petri dish and the biofilm exposed to UAS action or the water stream alone without ultrasonic activation with the water flow perpendicular to the surface. Representative photographs were taken for observation of gross biofilm removal. Each assay was performed in duplicate.

High-Speed Camera Assessment of S. mutans Removal Using an UAS from an Interproximal Space Model

To simulate the interproximal (IP) space of the teeth, 2 *S. mutans* biofilm-colonized slides were placed inside a rectangular plastic holder in parallel with a gap of 1 mm. The IP space holder was then placed under the device, and a high-speed camera (1,000 f/s; Motion Pro X3, IDT, Tallahassee, FL, USA) equipped with a Nikon (Tokyo, Japan) 105-mm f/2.8 VR G lens was used to capture the removal of the biofilm due to the UAS and the water stream alone without ultrasonic activation. In this assay, the water flow was run parallel to the biofilm. Representative videos can be found in the online supplementary material. Each experiment was performed in duplicate. High-speed videos were postprocessed with ImageJ software (National Institutes of Health, Bethesda, MD, USA). *S. mutans* biofilm clearance zone (CZ) was quantified by measuring the CZ area (A_{CZ}) in each frame every 300 ms. Then, the averaged A_{CZ} values (n = 2) with the relative SD were plotted as a function of the time. Statistical analysis was performed using an unpaired t test to compare normally distributed data means and difference considered significant where $P < 0.05$.

Surface Roughness Following UAS Exposure

Glass slides and hydroxyapatite (HA) coupons were exposed to the UAS for 10 s and 10 min continuously under the same conditions described above. Following exposure, the surface profiles were measured 2-dimensionally using the contact tracing system provided by the Taylor Hobson Talysurf 120L (Leicester, UK). The evaluation lengths were set at 5 and 40 mm for the HA coupons and glass slide, respectively, with a measurement speed of 0.5 mm/s. The primary raw data were filtered following the rules and procedures given in BS EN ISO 4288:1998. The characteristic wavelength of the profile filter λ_c was set at 0.8 and 0.08 mm for the HA coupons and glass slides, respectively. Surface roughness (R_a/µm) was determined in experimental triplicate, and statistical analysis was performed using an unpaired *t* test to compare normally distributed data means and difference considered significant where $P < 0.05$.

Removal of Biofilm from Artificial Rough Surface Using an UAS

Using a Loadpoint Microace 3 dicing saw (Swindon, UK), micro-grooves were cut into standard microscope glass slides to a uniform depth of 150 µm to a lattice configuration (period spacing: 500 µm × 760 µm, 760 µm × 1 mm, and 500 µm × 1 mm). The glass slides were then reduced in size to 15 mm × 15 mm using the dicing saw and rinsed in acetone and isopropanol to remove any organic residues, followed by dehydration at 200 °C for 30 min using a conventional oven. Following autoclaving at 121 °C for 20 min to sterilize, the slides were immersed in 4 mL of 10^6 CFU/mL and *S. mutans, A. naeslundii*, and *S. oralis* biofilms grown as described previously.

Following exposure to the UAS or water stream alone with the water flow positioned perpendicular to the surface, the slides were immersed in a primary fixative of 0.15 M sodium cacodylate buffer (pH 7.2) containing 3% glutaraldehyde and 0.15% Alcian blue 8GX for 24 h at 4 °C. A 1-h rinse in 0.15 M cacodylate buffer was performed at room temperature, and the biofilms were then postfixed in a secondary fixative containing 1% osmium tetraoxide in 0.15 M cacodylate buffer (pH 7.2) for 1 h. Following a further 1-h rinse in cacodylate buffer, the biofilms were dehydrated through an ascending ethanol series (50%, 70%, 80%, 95%, and 100% [twice]) prior to critical point drying and gold-palladium sputter coating and imaged using an FEI Quanta 200 Scanning Electron Microscope (Hillsboro, OR, USA).

Removal of S. mutans *Biofilms from a Typodont Model Using an UAS*

To re-create a realistic anatomical geometry of patient dental architecture in vitro, *S. mutans* biofilms were grown on the molars of a training typodont (A-PZ periodontal dental model 4030025; Frasaco GmbH, Tettnang, Germany) (Rmaile et al. 2014). The typodont teeth were autoclave sterilized and immersed in 5 mL of a 10^6 CFU/mL culture of *S. mutans* and

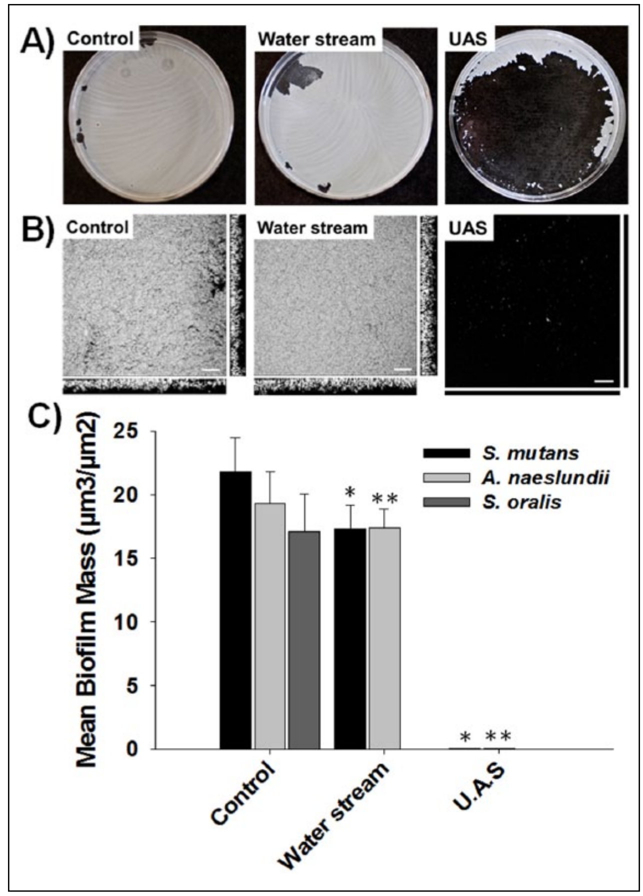

Figure 1. Removal of oral biofilms using an ultrasonically activated water stream (UAS). (**A**) Images show the zone of clearing of *Streptococcus mutans* UA159 biofilms grown in Petri dishes following 10-s exposure using the water stream alone without ultrasonic activation and the UAS, relative to an untreated control. In both cases, the water stream was positioned in the center of the plate. (**B**) Representative confocal scanning laser microscopy (CSLM) images of residual *S. mutans* UA159 biofilms following exposure to the UAS and water stream alone for 10 s, relative to an untreated control following Live/Dead Baclight fluorescent staining. Scale bars: 25 µm. (**C**) Graph shows COMSTAT analysis of residual mean biofilm mass with standard error bars of *S. mutans* UA159, *Actinomyces naeslundii* ATCC 12104, and *Streptococcus oralis* ATCC 9811 biofilms following a 10-s exposure to the UAS and the water stream alone as identified by Live/Dead Baclight fluorescent staining and CSLM (*n* = 8 with assay performed in duplicate). * and ** indicate corresponding data showing a statistically significant difference ($P < 0.01$).

biofilms grown as described previously. After this time, the teeth were removed using sterile tweezers and repositioned into the typodont and exposed to the UAS and water stream alone without ultrasonic activation with the water flow positioned perpendicular to the tooth crown. Following this, the teeth were removed from the typodont and immersed in 0.5% crystal violet (Sigma-Aldrich) for 10 min. Poststaining, the surface was dipped and gently rinsed in deionized water to remove excess stain prior to photographing to observed gross biofilm removal. To visualize removal from the teeth at the micro-scale, subsequent repeats were performed where the teeth were fixed as described above for scanning electron microscopy (SEM).

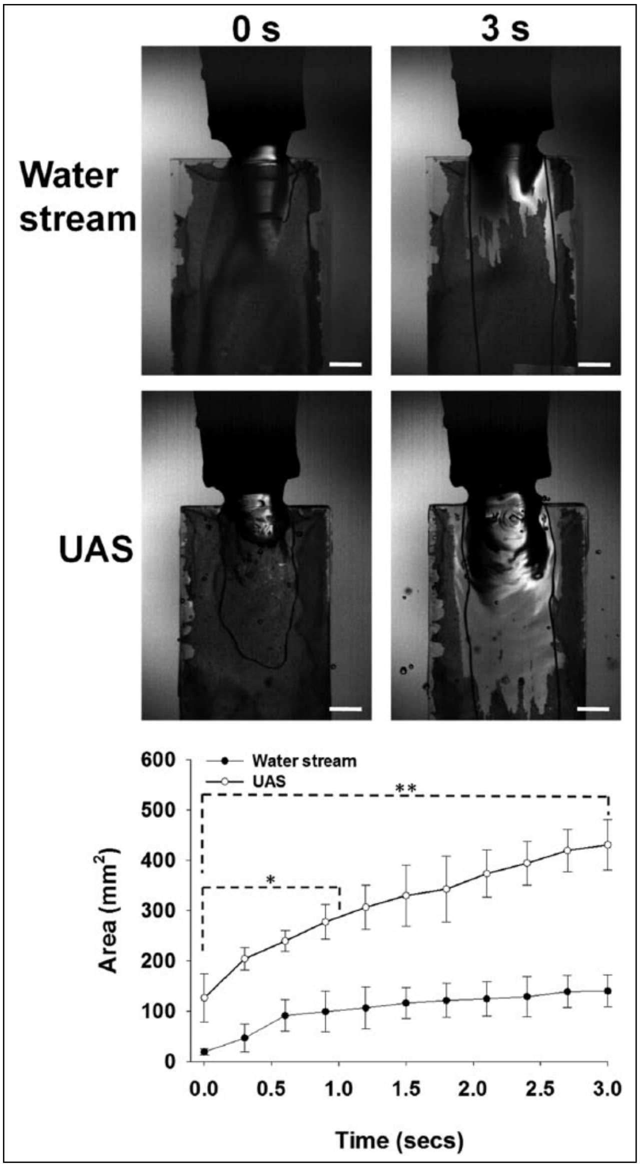

Figure 2. High-speed camera (1,000 f/s) imaging of *Streptococcus mutans* UA159 biofilm removal, using a ultrasonically activated water stream (UAS) and water stream alone, from glass slides placed in an interproximal space model. Images show representative frames from the high-speed camera at 0- and 3-s intervals. Scale bars: 5 mm. Graph shows the mean area of biofilm clearance against time following high-speed camera imaging of *S. mutans* biofilm removal using the UAS and water stream alone. Data points represent the mean of duplicate experimental repeats with standard error bars. * and ** represent data ranges of 0 to 1 s and 0 to 3 s, showing a statistically significant difference ($P < 0.5$).

Results

Gross *S. mutans* biofilm removal from Petri dishes was demonstrated as a larger (50.8-cm^2) zone of clearing from the center of the plate covering almost the entire plate diameter following 10-s exposure to the UAS, relative to the water stream alone without ultrasonic activation (3.5 cm^2; Fig. 1A). The water stream alone showed no removal of biofilm from the center of the plate at the initial water stream impact site and was

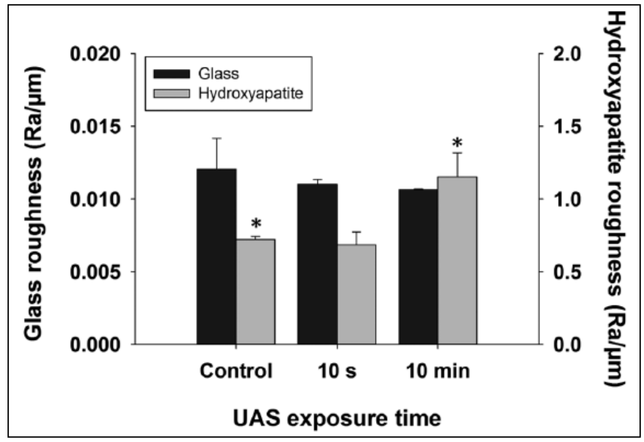

Figure 3. Surface profile (R_a/µm) following exposure of clean glass and hydroxyapatite surfaces to an ultrasonically activated water stream (UAS) for 10 s and 10 min. Data represent the mean of assays performed in experimental triplicate with standard deviation bars. Data points represent the mean of duplicate experimental repeats with standard error bars. * represents data showing a statistically significant difference ($P < 0.5$).

indistinguishable from untreated controls. Biofilm removal with the water stream alone was noted only at the edge of the plate, possibly due to water streaming around the plate edge.

A more detailed inspection by confocal microscopy showed that the UAS was significantly more effective at removing biofilms grown on simple flat surfaces (Fig. 1B) than the water stream alone. COMSTAT analysis of *S. mutans* biofilm removal showed that water stream treatment alone caused a 0.10 log reduction (20.7%) in biomass from 21.8 µm^3/µm^2 to 17.3 µm^3/µm^2 and a 0.17 log reduction (33.8%) in average thickness from 25.3 µm to 16.7 µm, although these reductions were not statistically different ($P = 0.24$). The UAS caused a further 2.3 log reduction in biomass to 0.08 µm^3/µm^2 (99.5% reduction compared with the untreated control) and a 2.9 log reduction in thickness to 0.02 µm (99.9% reduction), which was statistically significant ($P = 0.002$). Similarly, the water stream alone was unable to elicit a statistically significant reduction of *A. naeslundii* biofilms ($P = 0.645$) compared with the control, while biofilm removal with the UAS was significantly greater than the water stream alone ($P < 0.001$). However, the water stream alone, without UAS activation, resulted in a significant reduction in mean *S. oralis* biofilm mass relative to controls ($P = 0.001$), equivalent to a 99.95% reduction, suggesting weak surface attachment of *S. oralis* in this assay.

Further analysis using a high-speed camera of *S. mutans* biofilm removal from glass slides in a model mimicking the interproximal space showed a more rapid rate of biofilm removal during 0 to 3 s of UAS exposure relative to the water stream alone (Fig. 2; $P < 0.5$, $n = 2$). Within the first second of exposure, the biofilm clearance zone area (A_{CZ}) was 151 mm^2, relative to 80 mm^2 with the water stream alone. The A_{CZ} after a period of 3 s was 139.5 mm^2 (±32.03 mm^2, $n = 2$) and 430.4 (±50.34 mm^2, $n = 2$) for the water stream alone and the UAS, respectively. Representative high-speed camera videos can be found in the online supplementary material.

Analysis of the effect of a UAS on the underlying substratum was determined by 10-s and 10-min exposure to glass slides (used in Figs. 1 and 2) and HA coupons (Fig. 3). Exposure of glass slides to the UAS had no significant effect on R_a relative to the control (10 s: $P = 0.246$; 10 min: $P = 0.468$). There was also no statistically significant difference in R_a relative to controls of HA coupons exposed to the UAS for 10 s ($P = 0.544$). However, a 10-min exposure did elicit a significant increase in R_a ($P = 0.011$) from 0.72 to 1.15, equivalent to a 62.5% increase in surface R_a.

To further evaluate the effectiveness of UAS biofilm removal from a more complex surface, rough surfaces were created with various microgroove configurations and *S. mutans, A. naeslundii*, and *S. oralis* biofilms grown to demonstrate broad-spectrum bacterial species removal. SEM imaging following exposure to the water stream alone without ultrasonic activation showed no difference in residual biofilm relative to untreated controls (Fig. 4). However, a dramatic reduction in residual biofilm of all 3 bacterial strains was observed following treatment with the UAS relative to the water stream and untreated controls, with the rough surface showing no reduction in the efficacy of UAS mediated removal compared with previous assays on flat surfaces. Importantly, for *S. oralis*, this is in contrast to Figure 1, where the water stream alone was highly effective at biofilm removal, confirming UAS efficacy of hard-to-clean surfaces where the water stream alone was inefficient.

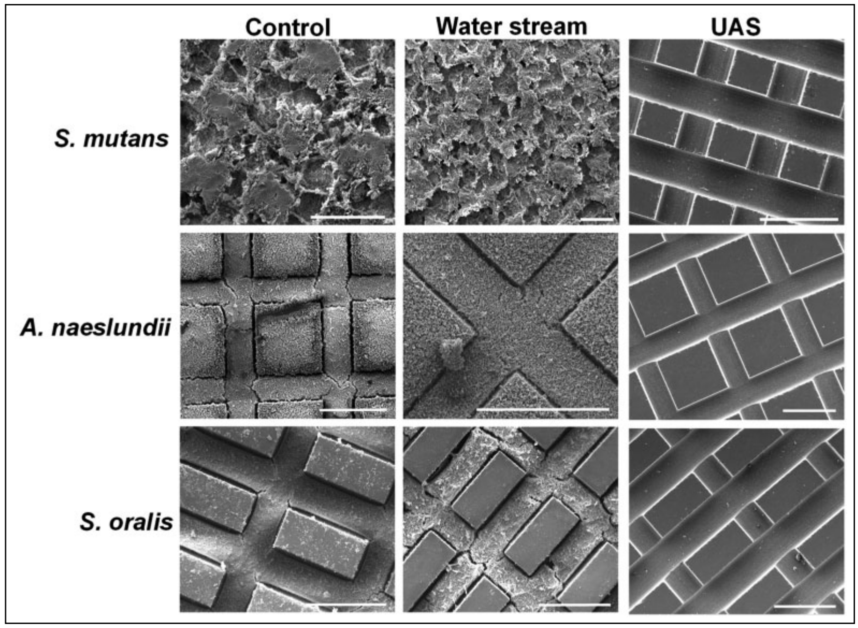

Figure 4. Scanning electron microscopy imaging of residual *Streptococcus mutans* UA159, *Actinomyces naeslundii* ATCC 12104, and *Streptococcus oralis* ATCC 9811 biofilms, grown on machine-etched glass slides to artificially and reproducibly mimic a rough surface, following exposure to the ultrasonically activated water stream (UAS) and water stream alone for 10 s, relative to untreated controls. Scale bars: 500 μm.

Similarly, the UAS was also effective at removing biofilm from teeth in a typodont training model representing a realistic patient dental architecture (Fig. 5). Crystal violet (CV) staining to assess gross biofilm removal again showed no noticeable difference between the water stream alone and control treatment groups, with a marked reduction in CV staining noted on teeth exposed to the UAS. SEM analysis imaging of the teeth to assess micro-scale removal of *S. mutans* biofilm revealed only occasional single cells visible in the areas exposed to the UAS. In contrast, the water stream alone showed comparable residual biofilm to the untreated control.

Discussion

As a key cariogenic species and a major risk factor for early childhood caries and future caries development, as well as its propensity to form biofilms, both in vitro and in vivo in the oral cavity, *S. mutans* was chosen as the model organism for the study (García-Godoy and Hicks 2008), in addition to *A. naeslundii* and *S. oralis*, to demonstrate broad-spectrum biofilm cleaning. Relative to a water stream flow of 2.1 L/min (±0.2 L/min), ultrasonic activation of the same stream at the same flow rate demonstrated a greater efficiency and rate of biofilm removal from a variety of increasingly complex surfaces, including, importantly, machine-etched slides to provide a consistent "rough" surface and molar teeth from a typodont model. Importantly, typodont model teeth effectively reproduce the normal dental architecture, including the complexity of the crown fissures where mechanical biofilm removal is more challenging and, combined with the IP space, are the most at-risk sites for caries development (Rugg-Gunn 2013).

UAS in a free water stream has several key and beneficial features that make it effective at biofilm removal (Leighton et al. 2011). First, effective cleaning can be achieved through pure water alone under ambient conditions and does not require chemical additives or the generation of high temperature. This is of added benefit as the lack of antimicrobial additives reduces the risk of antibiotic resistance developing and the risk to patient health due to the high doses of antimicrobials sometimes required to clear oral biofilm infections (Larsen and Fiehn 1996; Shani et al. 2000). Instead, the effectiveness of the UAS is achieved due to the utilization of the ultrasonically induced bubble activity and shear (Leighton et al. 2011). While it is known that, for some substrates and some bacterial species, the simple proximity of the passage of a nearby gas bubble (e.g., rising under buoyancy) can cause detachment (Gomez-Suarez et al. 2001), in this study, it is the ultrasonically induced volume and shape oscillations in the bubbles, as well as the associated shear, that produce the significant

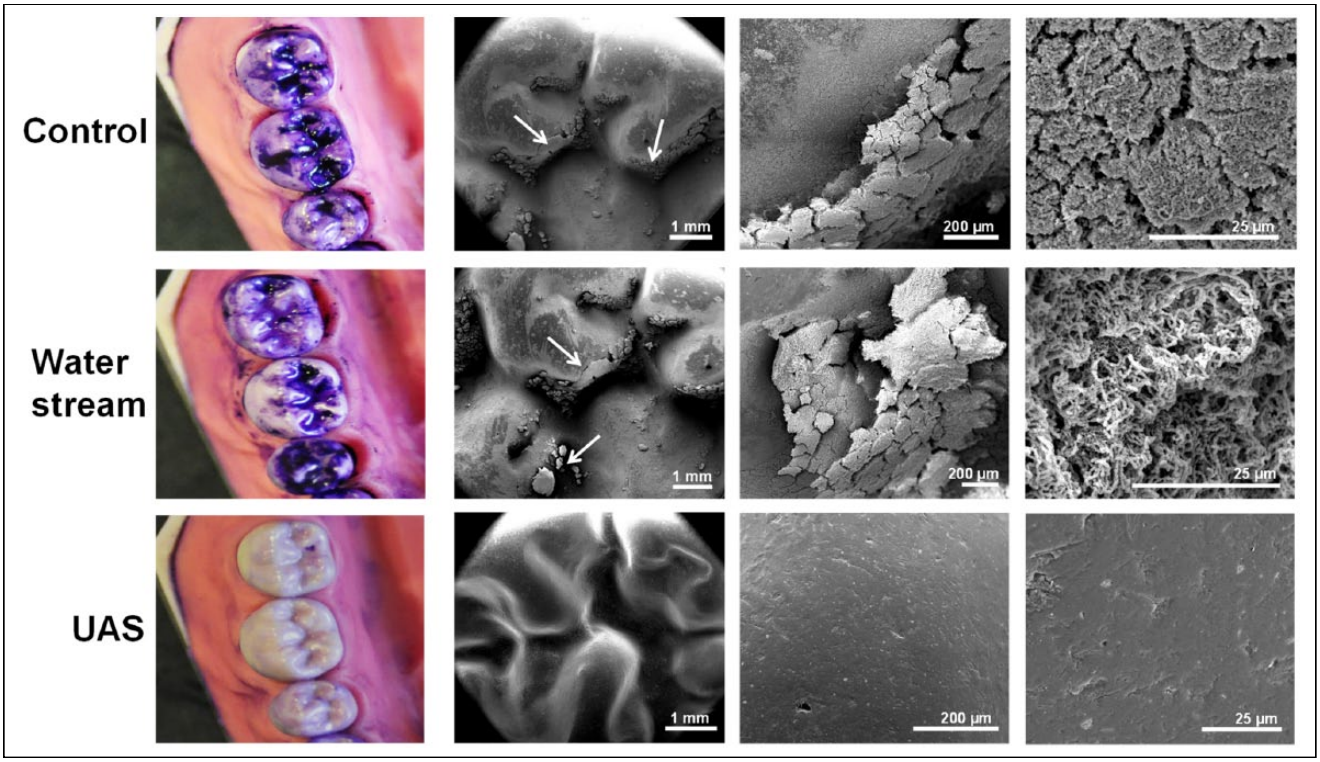

Figure 5. Representative images showing removal of *Streptococcus mutans* UA159 biofilms from molar teeth in a typodont training model, following a 10-s exposure to the ultrasonically activated water stream (UAS) and water stream alone, relative to untreated controls. Left-hand column panels show total residual biomass (blue/purple) as identified by crystal violet staining. Remaining panels show increasingly higher magnification scanning electron microscopy images of the crown surface. White arrows indicate residual *S. mutans* biofilm on low-magnification images. This figure is available in color online at http://jdr.sagepub.com.

removal effect (Leighton et al. 2011). Importantly, since the activated bubbles are in a free water stream, no direct contact between the device and the oral surface is required, facilitating access to hard-to-reach places. Second, the acoustic field causes the bubbles to move to crevices and such surface structures, preferentially cleaning features that are normally more difficult to clean (Leighton 1994; Offin et al. 2014). Consequently, due to the complex oral cavity topography, this approach has the potential to greatly contribute to improved oral hygiene. Third, the area of biofilm removal in this study was relevant in the context of dental hygiene and was achieved over the relatively short time period of a few seconds. The removal efficacy of laboratory-grown biofilms by UAS was similar to that of microburst technology in which high-velocity micro water drops generate high enough fluid shear to remove significant amounts of biofilm from an interproximal space model (Rmaile et al. 2014). However, the microdrops have the advantage of using minimal volumes of water. In addition, while not required for efficacy in this study, additives to the water reservoir, such as fluoride with proven anticaries properties, may further enhance not just the immediate cleaning efficacy but also long-term oral hygiene (Aspiras et al. 2010).

However, issues will need to be addressed regarding application of UAS to oral health care. Future work should address the influence of different surface materials (e.g., dental enamel and dentin) on UAS efficacy. In addition, the influence of the pellicle and salivary coating of a surface on UAS-mediated biofilm clearance needs to be assessed. Existing studies suggest that salivary mucins such as MUC5B decrease surface attachment and biofilm formation of *S. mutans*, and so UAS removal could be enhanced with a more representative oral environment (Frenkel and Ribbeck 2015). Careful consideration and future work will also be needed to assess the potential for tissue damage to the surrounding gingiva, but it is expected that these can be overcome by optimizing exposure time and power output to settings capable of maintaining the efficacy of the device and alleviating the risk of damage to the surrounding tissue. This is corroborated by data from this study where effective biofilm removal without a detrimental effect to the substratum was observed at short exposure times (10 s). Longer exposure times of 10 min did cause an increase in surface roughness on a hydroxyapatite surface; however, this should be put into context of other studies where exposure of 2 min to toothbrushing using certain dentrifices produced a much greater surface abrasion than observed with a 10-min UAS exposure (Pascaretti-Grizon et al. 2013). In addition, while the flow rate of 2.1 L/min used in this study provides good surface area coverage, there is the issue of requiring relatively large volumes of water, and thus miniaturization would be desirable. The current flow rate is higher than commercially available continuous or pulsed water irrigation shear-based removal devices that generally operate on the order of a few hundreds of mL/min (Rmaile et al. 2014). However, the use of a UAS represents a potentially practical and effective method for oral biofilm removal with the capacity to improve oral hygiene.

Author Contributions

R.P. Howlin, contributed to conception, design, data acquisition, analysis, and interpretation, drafted and critically revised the manuscript; S. Fabbri, contributed to data acquisition, analysis, and interpretation, critically revised the manuscript; D.G. Offin, N. Symonds, K.S. Kiang, R.J. Knee, D.C. Yoganantham, contributed to data acquisition, critically revised the manuscript; J.S. Webb, contributed to conception, critically revised the manuscript; P.R. Birkin, T.G. Leighton, contributed to conception, design, and data interpretation, critically revised the manuscript; P. Stoodley, conception, design, data analysis, and interpretation, critically revised the manuscript. All authors gave final approval and agree to be accountable for all aspects of the work.

Acknowledgments

This work was funded by the Royal Society Brian Mercer Award scheme. The authors thank Prof. J. Barton from The University of Southampton. Leighton and Birkin are named inventors of the ultrasonically activated water stream technology on the patent and on a standard licence deal between the University of Southampton and Ultrawave Ltd. The other authors declare no potential conflicts of interest with respect to the authorship and/or publication of this article.

References

Aas JA, Paster BJ, Stoke LN, Olsen I, Dewhirst FE. 2005. Defining the normal bacterial flora of the oral cavity. J Clin Microbiol. 43(11):5721–5732.

Aspiras M, Stoodley P, Nistico L, Longwell M, de Jager M. 2010. Clinical implications of power toothbrushing on fluoride delivery: effects on biofilm plaque metabolism and physiology. Int J Dent. 2010:651869.

Brading MG, Marsh PD. 2003. The oral environment: the challenge for antimicrobials in oral care products. Int Dent J. 53(6 Suppl 1):353–362.

Doinikov AA. 2001. Translational motion of two interacting bubbles in a strong acoustic field. Phys Rev E Stat Nonlin Soft Matter Phys. 64(2 Pt 2):026301.

Falsetta ML, Klein MI, Lemos JA, Silva BB, Agidi S, Scott-Anne KK, Koo H. 2012. Novel antibiofilm chemotherapy targets exopolysaccharide synthesis and stress tolerance in Streptococcus mutans to modulate virulence expression in vivo. Antimicrob Agents Chemother. 56(12):6201–6211.

Forssten SD, Björklund M, Ouwehand AC. 2010. *Streptococcus mutans*, caries and simulation models. Nutrients. 2(3):290–298.

Frenkel ES, Ribbeck K. 2015. Salivary mucins protect surfaces from colonization by cariogenic bacteria. Appl Environ Microbiol. 81(1)332–338.

García-Godoy F, Hicks MJ. 2008. Maintaining the integrity of the enamel surface: the role of dental biofilm, saliva and preventive agents in enamel demineralization and remineralization. J Am Dent Assoc. 139(Suppl 2):25S–34S.

Gomez-Suarez C, Busscher HJ, van der Mei HC. 2001. Analysis of bacterial detachment from substratum surfaces by the passage of air-liquid interfaces. Appl Environ Microbiol. 67(6):2531–2537.

Halford A, Ohl CD, Azarpazhooh A, Basrani B, Friedman S, Kishen A. 2012. Synergistic effect of microbubble emulsion and sonic or ultrasonic agitation on endodontic biofilm in vitro. J Endod. 38(11):1530–1534.

Heydorn A, Nielsen AT, Hentzer M, Sternberg C, Givskov M, Ersbøll BK, Molin S. 2000. Quantification of biofilm structures by the novel computer program COMSTAT. Microbiology. 146(10):2395–2407.

Larsen T, Fiehn NE. 1996. Resistance of *Streptococcus sanguis* biofilms to antimicrobial agents. Apmis. 104(4):280–284.

Lea SC, Price GJ, Walmsley AD. 2005. A study to determine whether cavitation occurs around dental ultrasonic scaling instruments. Ultrason Sonochem. 12(3):233–236.

Leighton TG. 1994. The acoustic bubble. New York (NY): Academic Press.

Leighton TG, Vian CJB, Birkin PR, inventors; University of Southampton, assignee. 2011. Cleaning apparatus and method, and monitoring thereof. Patent PCT/EP2010/062448.

Lemos JA, Quivey RG Jr, Koo H, Abranches J. 2013. *Streptococcus mutans:* a new Gram-positive paradigm? Microbiology. 159(Pt 3):436–445.

Marsh PD. 2003. Are dental diseases examples of ecological catastrophes? Microbiology. 149(Pt 2):279–294.

Marsh PD. 2010. Controlling the oral biofilm with antimicrobials. J Dent. 38(Suppl 1):S11–S15.

Offin DG, Birkin PR, Leighton TG. 2014. An electrochemical and high-speed imaging study of micropore decontamination by acoustic bubble entrapment. Phys Chem Chem Phys. 16(10):4982–4989.

O'Leary R, Sved AM, Davies EH, Leighton TG, Wilson M, Kieser JB. 1997. The bactericidal effects of dental ultrasound on *Actinobacillus actinomycetemcomitans* and *Porphyromonas gingivalis*. J Clin Periodontol. 24(6):432–439.

Parini MR, Pitt WG. 2005. Removal of oral biofilms by bubbles: the effect of bubble impingement angle and sonic waves. J Am Dent Assoc. 136(12):1688–1693.

Parini MR, Pitt WG. 2006. Dynamic removal of oral biofilms by bubbles. Colloids Surf B Biointerfaces. 52(1):39–46.

Pascaretti-Grizon F, Mabillaeu G, Chappard D. 2013. Abrasion of 6 dentrifices measured by vertical scanning interference microscopy. J Appl Oral Sci. 21(5):475–481.

Rmaile A, Carugo D, Capretto L, Aspiras M, De Jager M, Ward M, Stoodley P. 2014. Removal of interproximal dental biofilms by high-velocity water microdrops. J Dent Res. 93(1):68–73.

Rooney JA. 1970. Hemolysis near an ultrasonically pulsating gas bubble. Science. 169(3948):869–871.

Rugg-Gunn A. 2013. Dental caries: strategies to control this preventable disease. Acta Med Acad. 42(2):117–130.

Shani S, Friedman M, Steinberg D. 2000. The anticariogenic effect of amine fluorides on *Streptococcus sobrinus* and glucosyltransferase in biofilms. Caries Res. 34(3):260–267.

Stricker L, Dollet B, Fernandez Rivas D, Lohse D. 2013. Interacting bubble clouds and their sonochemical production. J Acoust Soc Am. 134(3):1854–1862.

von Ohle C, Gieseke A, Nistico L, Decker EM, deBeer D, Stoodley P. 2010. Real-time microsensor measurement of local metabolic activities in ex vivo dental biofilms exposed to sucrose and treated with chlorhexidine. Appl Environ Microbiol. 76(7):2326–2334.

Zaura E, Keijser BJ, Huse SM, Crielaard W. 2009. Defining the healthy "core microbiome" of oral microbial communities. BMC Microbiol. 15(9):259.